# Multiple Soliton Asymptotics in a Spin-1 Bose–Einstein Condensate

Zhong-Zhou Lan(兰中周)*

*School of Computer Information Management, Inner Mongolia University of Finance and Economics, Hohhot 010070, China*

(Received 19 July 2024; accepted manuscript online 23 August 2024)

Spinor Bose–Einstein condensates (BECs) are formed when atoms in the multi-component BECs possess single hyperfine spin states but retain internal spin degrees of freedom. This study concentrates on a (1+1)-dimensional three-couple Gross–Pitaevskii system to depict the macroscopic spinor BEC waves within the mean-field approximation. Regarding the distribution of the atoms corresponding to the three vertical spin projections, a known binary Darboux transformation is utilized to derive the $N$ matter-wave soliton solutions and triple-pole matter-wave soliton solutions on the zero background, where $N$ is a positive integer. For those multiple matter-wave solitons, the asymptotic analysis is performed to obtain the algebraic expressions of the soliton components in the $N$ matter-wave solitons and triple-pole matter-wave solitons. The asymptotic results indicate that the matter-wave solitons in the spinor BECs possess the property of maintaining their energy content and coherence during the propagation and interactions. Particularly, in the $N$ matter-wave solitons, each soliton component contributes to the phase shifts of the other soliton components; and in the triple-pole matter-wave solitons, stable attractive forces exist between the different matter-wave soliton components. Those multiple matter-wave solitons are graphically illustrated through three-dimensional plots, density plot and contour plot, which are consistent with the asymptotic analysis results. The present analysis may provide the explanations for the complex natural mechanisms of the matter waves in the spinor BECs, and may have potential applications in designs of atom lasers, atom interferometry and coherent atom transport.

DOI: 10.1088/0256-307X/41/9/090501

Bose–Einstein condensates (BECs) refer to states of matter formed when a dilute gas of bosons is cooled to temperatures very close to absolute zero.[1–7] Under such conditions, a significant fraction of bosons occupy the lowest quantum state, allowing quantum effects to become apparent on a macroscopic scale.[8–12] Numerous studies have highlighted two key features of BECs:[13–15] Firstly, the intrinsic properties of a BEC system, such as the strength of interatomic interactions, can be manipulated using magnetic fields and lasers. Secondly, the mean-field theory provides an accurate description of BECs in dilute atomic gases. BECs are considered to have potential applications in interferometry, quantum simulations, and development of novel sensors.[16,17]

When atoms in multi-component BECs possess single hyperfine spin states but retain internal spin degrees of freedom, they form spinor BECs.[18,19] Notably, when spinor BECs are confined in an optical trap without external magnetic fields, the spin of the atoms is free to evolve.[20] Both experimental and theoretical studies have revealed a wealth of unique phenomena in spinor BECs (compared to single-component BECs), such as polar-to-ferromagnetic phase transitions, quantum knots, condensation of magnon excitations, and various types of nonlinear excitations including dark/bright solitons, soliton complexes, rogue waves, and vortices.[21–23]

When spinor BECs are confined by an optical dipole trap and the scattering lengths satisfy a specific ratio, the three internal states $m_{\rm F} = 1, 0, -1$ of the spinor BECs become degenerate in the same spin-1 ($F = 1$) hyperfine state, where $m_{\rm F}$ is the magnetic quantum number.[24] Under these conditions, the distribution of atoms is described by the three-component macroscopic BEC wave functions $\psi_{-1}$, $\psi_0$, $\psi_1$, corresponding to the three vertical spin projections $m_{\rm F} = -1, 0, 1$, respectively.[25] Within the mean-field approximation, a (1+1)-dimensional three-component Gross–Pitaevskii (GP) system has been derived,[24–31]

$$\begin{aligned}
&i\hbar\psi_{\pm1,T} + \frac{\hbar^2}{2m}\psi_{\pm1,XX} - (d_0+d_2)(|\psi_{\pm1}|^2 + |\psi_0|^2)\psi_{\pm1} \\
&- (d_0-d_2)|\psi_{\mp1}|^2\psi_{\pm1} - d_2\psi^*_{\mp1}\psi_0^2 = 0, \\
&i\hbar\psi_{0,T} + \frac{\hbar^2}{2m}\psi_{0,XX} - (d_0+d_2)(|\psi_{+1}|^2 + |\psi_{-1}|^2)\psi_0 \\
&- d_0|\psi_0|^2\psi_0 - 2d_2\psi_0^*\psi_1\psi_{-1} = 0,
\end{aligned} \tag{1}$$

where $X$ and $T$ are the scaled spatial and time variables; $\psi_{-1}$, $\psi_0$, and $\psi_1$ are the three complex condensate wave functions of $X$ and $T$ denoting the atom states; $i = \sqrt{-1}$, $\hbar$ is the reduced Planck constant, $m$ is the atomic mass, the asterisk * denotes the complex conjugate; the subscripts $X$, $T$ denote the corresponding partial derivatives; $d_0$ and $d_2$ represent the spin-preserving and spin-exchange interactions. Here, $d_0 = (g_0 + 2g_2)/3$, $d_2 = (g_2 - g_0)/3$, the

*Corresponding author. Email: zhongzhou-lan@buaa.edu.cn
© 2024 Chinese Physical Society and IOP Publishing Ltd

coupling constants

$$g_f = \frac{4\hbar^2 a_f}{m a_\perp^2}\frac{1}{1-Ka_f/a_\perp}, \quad f=0,2,$$

$a_f$ is the s-wave scattering length in the channel with the total hyperfine spin $f$, $a_\perp$ denotes the size of the transverse ground state, $K=-\zeta(\frac{1}{2})=1.4603\cdots$, and $\zeta$ is the Riemann zeta-function.[24,25]

A reduction of system (1) has been explored under the conditions $d_0=d_2=-d<0$ (i.e., $2g_0=-g_2>0$), corresponding to the attractive spin-preserving and ferromagnetic spin-exchange interactions.[32–35] The above reduction has been satisfied by imposing a condition on the scattering lengths, $a_\perp=3Ka_0a_2/(2a_0+a_2)$.[27] Such a strong transversal confinement has been realized in a 2D optical lattice where $a_\perp$ is approximately tens of nanometers.[29]

By employing the transformation $(\psi_1,\psi_0,\psi_{-1})\to(\phi_1,\sqrt{2}\phi_0,\phi_{-1})$ and variable scalings $t=Td/\hbar$, $x=\sqrt{2md}X/\hbar$, system (1) can be reformulated into[32–38]

$$\begin{aligned}
&i\phi_{1,t}+\phi_{1,xx}+2(|\phi_1|^2+2|\phi_0|^2)\phi_1+2\phi_{-1}^*\phi_0^2=0,\\
&i\phi_{0,t}+\phi_{0,xx}+2(|\phi_1|^2+|\phi_0|^2+|\phi_{-1}|^2)\phi_0+2\phi_0^*\phi_1\phi_{-1}=0,\\
&i\phi_{-1,t}+\phi_{-1,xx}+2(|\phi_{-1}|^2+2|\phi_0|^2)\phi_{-1}+2\phi_1^*\phi_0^2=0. \quad (2)
\end{aligned}$$

For system (2), a multi-fold binary Darboux transformation (DT), double-pole mixed solitons and the corresponding asymptotic analysis have been presented before.[32] Some solitons, breathers and rogue waves have been identified and analyzed in different contexts.[33] High-order rogue waves and mixed interaction patterns have been investigated.[34] Bright-dark-bright and bright-bright-bright matter rogue waves have been studied.[35] Inverse scattering transform and scattering behaviors of the matter waves have been derived.[36] Managements of the matter rogue waves have been discussed.[37] Long-time asymptotics has been investigated.[38]

Matter-wave solitons, a type of nonlinear waves characterized by their ability to propagate undistorted due to a balance between nonlinearity and dispersion, has been observed in BECs.[39–43] So far, three primary types of solitons have been identified in BECs: Bright solitons, which are the localized regions of the higher density that form in the BECs with the attractive interactions, have been observed in the lithium BECs.[39,40] Dark solitons, which are the localized regions of lower density (or "holes") that form in the BECs with the repulsive interactions, have been observed in the sodium and rubidium BECs.[41,42] Gap solitons, which occur in the BECs trapped in periodic potentials (optical lattices) and can exist in gaps of band structures of lattices.[43] Matter-wave solitons in atom optics with the internal spin degrees of freedom may be utilized in development of atom lasers, atom interferometry, quantum information processing and coherent atom transport.[44,45]

However, to our knowledge, multiple matter-wave soliton asymptotics for system (2) in spinor Bose–Einstein condensates, including the $N$-soliton and triple-pole-soliton asymptotics, where $N$ is a positive integer, have not yet been reported. Via symbolic computation,[46–51] we will perform asymptotic analysis on the $N$-soliton solutions and triple-pole-soliton solutions for system (2). Expressions and dynamic properties of those multiple interacting matter-wave solitons will be discussed. Finally, we will draw our conclusions.

*Multiple Matter-Wave Soliton Asymptotics for System (2).* For matter waves in BECs, we consider the dynamics of the interacting $N$ solitons and triple-pole solitons.

*$N$-soliton Asymptotics and Corresponding Example Verification.* For some nonlinear evolution equations/systems, the binary DT method has been considered to be effective for obtaining the $N$-fold solutions that depict the multiple interacting nonlinear waves.

Lax pair is a prerequisite for the binary DT method. A Lax pair for system (2) has been presented,[27,32]

$$\begin{aligned}
&\Gamma_x=U\Gamma, \quad \Gamma_t=V\Gamma, \quad U=iJ\lambda+U_0,\\
&V=2iJ\lambda^2+2U_0\lambda+iJ(U_0^2-U_{0,x}), \qquad (3)
\end{aligned}$$

where

$$J=\mathrm{diag}(-1,-1,1,1),\ U_0=\begin{pmatrix}0 & \Phi\\ -\Phi^\dagger & 0\end{pmatrix},\ \Phi=\begin{pmatrix}\phi_1 & \phi_0\\ \phi_0 & \phi_{-1}\end{pmatrix},$$

where $\Gamma$ is a $4\times1$ vector eigenfunction, $\lambda$ is the complex spectral parameter, and the superscript † denotes the Hermitian conjugate. For Lax Pair (3), the compatibility condition $U_t-V_x+UV-VU=0$ leads to system (2).

Generally, solitons appear on the zero background. Hence, we set the seed solutions for system (2) as $\phi_{-1}=\phi_0=\phi_1=0$, i.e., the zero background. Assuming that $\Gamma_j$'s are $N$ distinct eigenfunctions of Lax Pair (3) at the complex spectral parameter $\lambda_j$ and the zero background,

$$\begin{aligned}
&\Gamma_j=\begin{pmatrix}\gamma_{1,j}\\ \gamma_{2,j}\\ \gamma_{3,j}\\ \gamma_{4,j}\end{pmatrix}=\begin{pmatrix}e^{\theta_j}\\ e^{\theta_j}\\ e^{-\theta_j}\\ e^{-\theta_j}\end{pmatrix}, \quad \theta_j=-i\lambda_j x-2i\lambda_j^2 t,\\
&\theta_{j,\mathrm{R}}=\lambda_{j,\mathrm{C}}(x+4\lambda_{j,\mathrm{R}}t),\ \theta_{j,\mathrm{C}}=-\lambda_{j,\mathrm{R}}x+2(\lambda_{j,\mathrm{C}}^2-\lambda_{j,\mathrm{R}}^2)t, \qquad (4)
\end{aligned}$$

where the subscript R denotes the real part, the subscript C denotes the complex part, and $j=1,2,3,\ldots,N$. Generally in the $N$-soliton solutions on the zero background obtained via the binary DT method, each spectral parameter corresponds to a soliton component.

With the aid of the binary DT in Ref. [32], we derive the $N$-soliton solutions for system (2) as

$$\begin{aligned}
&\phi_1[N]=-2iX_1\Omega^{-1}X_3^\dagger=2i\frac{\begin{vmatrix}\Omega & X_3^\dagger\\ X_1 & 0\end{vmatrix}}{|\Omega|},\\
&\phi_0[N]=-2iX_1\Omega^{-1}X_4^\dagger=2i\frac{\begin{vmatrix}\Omega & X_4^\dagger\\ X_1 & 0\end{vmatrix}}{|\Omega|},\\
&\phi_{-1}[N]=-2iX_2\Omega^{-1}X_4^\dagger=2i\frac{\begin{vmatrix}\Omega & X_3^\dagger\\ X_2 & 0\end{vmatrix}}{|\Omega|}, \qquad (5)
\end{aligned}$$

where $[N]$ denotes the $N$th-order iteration, the superscript "$-1$" denotes the inverse matrix, $\Omega$ is an $N\times N$ matrix with $\Omega_{j,k}=\Gamma_j^*\Gamma_k/(\lambda_k-\lambda_j^*)$, $j,k=1,2,\ldots,N$,

$X = (\Gamma_1\ \Gamma_2\ \cdots\ \Gamma_N)$, and $X_\iota$ ($\iota = 1, 2, 3, 4$) is the $\iota$th-row of $X$.

It should be noted that many intermediate parameters have been used to generate $N$-soliton solutions (5) via the binary DT method. On the one hand, since system (2) is a particular integrable case of system (1), we believe that the existence of the Lax Pair (3), eigenfunction (4) and binary DT is an intrinsic property of system (2). Thus, the intermediate parameters involved, which lack physical explanations, do not affect the conclusions we will draw later. On the other hand, in the BECs, the spectral parameters $\lambda_j$'s for the nonlinear equations/systems have been generally related to the energy levels and momentum of the condensate. Particularly for the soliton solutions, those spectral parameters determine the binding energies of the solitons, representing the energies required to form the soliton from the condensate.

Moreover, we obtain

$$\begin{aligned}
&\Omega_{j,k} = \frac{2(e^{\theta_j^*+\theta_k} + e^{-\theta_j^*-\theta_k})}{\lambda_k - \lambda_j^*},\\
&X_1 = X_2 = (e^{\theta_1}\ \ e^{\theta_2}\ \ \ldots\ \ e^{\theta_N}),\\
&X_3^\dagger = X_4^\dagger = (e^{-\theta_1^*}\ \ e^{-\theta_2^*}\ \ \ldots\ \ e^{-\theta_N^*})^{\mathrm{T}}.
\end{aligned} \tag{6}$$

Through multiplying the $j$th row ($j = 1, 2, \ldots, N$) of $|\Omega|$ and $\begin{vmatrix} \Omega & X_3^\dagger \\ X_1 & 0 \end{vmatrix}$ by $e^{\theta_j^*}$, and multiplying the $k$th column ($k = 1, 2, \ldots, N$) of $|\Omega|$ and $\begin{vmatrix} \Omega & X_3^\dagger \\ X_1 & 0 \end{vmatrix}$ by $e^{\theta_k}$, we transform $N$-soliton solutions (5) into the following form:

$$\phi_1[N] = \phi_0[N] = \phi_{-1}[N] = 2i\frac{\begin{vmatrix} \widehat{\Omega} & \widehat{X}_3^\dagger \\ \widehat{X}_1 & 0 \end{vmatrix}}{|\widehat{\Omega}|}, \tag{7}$$

where

$$\begin{aligned}
&\widehat{\Omega} = (\widehat{\Omega}_{j,k})_{N\times N},\quad \widehat{\Omega}_{j,k} = \frac{2[e^{2(\theta_j^*+\theta_k)}+1]}{\lambda_k - \lambda_j^*},\\
&\widehat{X}_1 = (e^{2\theta_1}\ \ e^{2\theta_2}\ \ \ldots\ \ e^{2\theta_N}),\quad \widehat{X}_3^\dagger = (1\ \ 1\ \ \ldots\ \ 1)^{\mathrm{T}}.
\end{aligned}$$

We denote the soliton component related to the spectral parameter $\lambda_\omega$ as the $\omega$-th soliton component. Eigenfunctions (4) reveal that the $\omega$th soliton propagates with the velocity $V_\omega = -4\lambda_{\omega,R}$. Without loss of generality, we set $\lambda_{j,\mathrm{C}} > 0$, $\lambda_{1,\mathrm{R}} > \lambda_{2,\mathrm{R}} > \cdots > \lambda_{N,R}$, i.e., velocities of those $N$ soliton components on the $x$–$t$ plane increase sequentially with the sequence number.

Under the given assumptions, when $t \to -\infty$, along the characteristic line $x + 4\lambda_{\omega,R}t = \text{const}$, we observe that $\theta_{1,\mathrm{R}}, \theta_{2,\mathrm{R}}, \ldots, \theta_{\omega-1,R} \to -\infty$; $\theta_{\omega+1,R}, \theta_{\omega+2,R}, \ldots, \theta_{N,R} \to +\infty$, where $\omega = 1, 2, 3, \ldots, N$. Hence, for $|\widehat{\Omega}|$, along the characteristic line $x + 4\lambda_{\omega,R}t = \text{const}$, we extract $e^{2\theta_{\rho_1}^*}$ from the $\rho_1$th row of $|\widehat{\Omega}|$, and extract $e^{2\theta_{\rho_1}}$ from the $\rho_1$th column of $|\widehat{\Omega}|$, where $\rho_1 = \omega+1, \omega+2, \ldots, N$, then obtain

$$\lim_{t\to-\infty}|\widehat{\Omega}| = (-2)^N e^{4(\theta_{\omega+1,R}+\theta_{\omega+2,R}+\cdots+\theta_{N,R})}|\widehat{\Omega}^-|,$$

$$|\widehat{\Omega}^-| = \begin{vmatrix}
\frac{1}{\lambda_1^*-\lambda_1} & \cdots & \frac{1}{\lambda_1^*-\lambda_{\omega-1}} & \frac{1}{\lambda_1^*-\lambda_\omega} & 0 & \cdots & 0\\
\vdots & \ddots & \vdots & \vdots & \vdots & \ddots & \vdots\\
\frac{1}{\lambda_{\omega-1}^*-\lambda_1} & \cdots & \frac{1}{\lambda_{\omega-1}^*-\lambda_{\omega-1}} & \frac{1}{\lambda_{\omega-1}^*-\lambda_\omega} & 0 & \cdots & 0\\
\frac{1}{\lambda_\omega^*-\lambda_1} & \cdots & \frac{1}{\lambda_\omega^*-\lambda_{\omega-1}} & \frac{e^{2(\theta_\omega^*+\theta_\omega)}+1}{\lambda_\omega^*-\lambda_\omega} & \frac{e^{2\theta_\omega^*}}{\lambda_\omega^*-\lambda_{\omega+1}} & \cdots & \frac{e^{2\theta_\omega^*}}{\lambda_\omega^*-\lambda_N}\\
0 & \cdots & 0 & \frac{e^{2\theta_\omega}}{\lambda_{\omega+1}^*-\lambda_\omega} & \frac{1}{\lambda_{\omega+1}^*-\lambda_{\omega+1}} & \cdots & \frac{1}{\lambda_{\omega+1}^*-\lambda_N}\\
\vdots & \ddots & \vdots & \vdots & \vdots & \ddots & \vdots\\
0 & \cdots & 0 & \frac{e^{2\theta_\omega}}{\lambda_N^*-\lambda_\omega} & \frac{1}{\lambda_N^*-\lambda_{\omega+1}} & \cdots & \frac{1}{\lambda_N^*-\lambda_N}
\end{vmatrix}. \tag{8}$$

We operate the same procedure for $\begin{vmatrix} \widehat{\Omega} & \widehat{X}_3^\dagger \\ \widehat{X}_1 & 0 \end{vmatrix}$ as the above $|\widehat{\Omega}|$, and obtain

$$\begin{aligned}
\lim_{t\to-\infty}\begin{vmatrix} \widehat{\Omega} & \widehat{X}_3^\dagger \\ \widehat{X}_1 & 0 \end{vmatrix} &= (-2)^{N-1}e^{4(\theta_{\omega+1,R}+\theta_{\omega+2,R}+\cdots+\theta_{N,R})}\\
&\quad\cdot\begin{vmatrix} \widehat{\Omega}^- & (\widehat{X}_3^-)^\dagger \\ \widehat{X}_1^- & 0 \end{vmatrix},\\
\widehat{X}_1^- &= \Big(\underbrace{0,\ldots,0}_{\omega-1}, e^{2\theta_\omega}, \underbrace{1,\ldots,1}_{N-\omega}\Big),\\
(\widehat{X}_3^-)^\dagger &= \Big(\underbrace{1,\ldots,1}_{\omega}, 0, \ldots, 0\Big)^{\mathrm{T}}.
\end{aligned} \tag{9}$$

According to the Laplace theorem, we split the elements in the $\omega$th column of $|\widehat{\Omega}^-|$, and then directly obtain

$$\begin{aligned}
|\widehat{\Omega}^-| &= C(1,\ldots,\omega)C(\omega+1,\ldots,N)\\
&\quad + C(1,\ldots,\omega-1)C(\omega,\ldots,N)e^{4\theta_{\omega,R}}\\
&= \frac{1}{\lambda_\omega - \lambda_\omega^*}C(1,\ldots,\omega-1)C(\omega+1,\ldots,N)\\
&\quad\cdot\Big(\prod_{l=1}^{\omega-1}\frac{|\lambda_\omega^*-\lambda_l^*|^2}{|\lambda_\omega^*-\lambda_l|^2} + e^{4\theta_{\omega,R}}\prod_{l=\omega+1}^{N}\frac{|\lambda_\omega-\lambda_l|^2}{|\lambda_\omega-\lambda_l^*|^2}\Big),
\end{aligned} \tag{10}$$

where $C(m_1, m_1+1,\ldots, m_2-1, m_2) = \mathrm{Det}(\frac{1}{\lambda_{n_1}^*-\lambda_{n_2}})_{m_1\le n_1,\, n_2\le m_2}$ is the determinant of the Cauchy matrix, and $m_1$ and $m_2$ are the integers satisfying $1 \le m_1 < m_2 \le N$.

For $\begin{vmatrix} \widehat{\Omega}^- & (\widehat{X}_3^-)^\dagger \\ \widehat{X}_1^- & 0 \end{vmatrix}$, we do the Laplace expansion on its $(N+1)$th column and directly obtain

$$\begin{vmatrix} \widehat{\Omega}^{-} & (\widehat{X}_3^{-})^{\dagger} \\ \widehat{X}_1^{-} & 0 \end{vmatrix} = (-1)^{N+\omega+1} \begin{vmatrix} \frac{1}{\lambda_1^*-\lambda_1} & \cdots & \frac{1}{\lambda_1^*-\lambda_{\omega-1}} & 1 \\ \vdots & \ddots & \vdots & \vdots \\ \frac{1}{\lambda_{\omega-1}^*-\lambda_1} & \cdots & \frac{1}{\lambda_{\omega-1}^*-\lambda_{\omega-1}} & 1 \\ \frac{1}{\lambda_\omega^*-\lambda_1} & \cdots & \frac{1}{\lambda_\omega^*-\lambda_{\omega-1}} & 1 \end{vmatrix} \begin{vmatrix} \frac{e^{2\theta_\omega}}{\lambda_{\omega+1}^*-\lambda_\omega} & \frac{1}{\lambda_{\omega+1}^*-\lambda_{\omega+1}} & \cdots & \frac{1}{\lambda_{\omega+1}^*-\lambda_N} \\ \vdots & \vdots & \ddots & \vdots \\ \frac{e^{2\theta_\omega}}{\lambda_N^*-\lambda_\omega} & \frac{1}{\lambda_N^*-\lambda_{\omega+1}} & \cdots & \frac{1}{\lambda_N^*-\lambda_N} \\ e^{2\theta_\omega} & 1 & \cdots & 1 \end{vmatrix}$$
$$= (-1)^{N+\omega+1} \prod_{l=1}^{\omega-1} \Big(\frac{\lambda_\omega^*-\lambda_l^*}{\lambda_\omega^*-\lambda_l}\Big) \prod_{l=\omega+1}^{N} \Big(\frac{\lambda_\omega-\lambda_l}{\lambda_\omega-\lambda_l^*}\Big) C(1, \ldots, \omega-1) C(\omega+1, \ldots, N) e^{2\theta_\omega}. \tag{11}$$

Finally, when $t \to -\infty$, we obtain the expression of the $\omega$th asymptotic soliton component as

$$|\phi_1[N]| = |\phi_0[N]| = |\phi_{-1}[N]|$$
$$= |\lambda_{\omega,C}| \operatorname{sech}\Big(2\theta_{\omega,R} + \frac{1}{2}\ln\Upsilon_\omega\Big), \tag{12}$$

where

$$\Upsilon_\omega = \prod_{l=1}^{\omega-1} \frac{|\lambda_\omega-\lambda_l^*|^2}{|\lambda_\omega-\lambda_l|^2} \prod_{l=\omega+1}^{N} \frac{|\lambda_\omega-\lambda_l|^2}{|\lambda_\omega-\lambda_l^*|^2}.$$

Similarly, when $t \to +\infty$, along the characteristic line $x + 4\lambda_{\omega,R}t = \text{const}$, we observe that $\theta_{1,\mathrm{R}}, \theta_{2,\mathrm{R}}, \ldots, \theta_{\omega-1,R} \to +\infty$; $\theta_{\omega+1,R}, \theta_{\omega+2,R}, \ldots, \theta_{N,R} \to -\infty$, where $\omega = 1, 2, 3, \ldots, N$. Hence, we extract $e^{2\theta_{\rho_2}^*}$ from the $\rho_2$th row of $|\widehat{\Omega}|$, and extract $e^{2\theta_{\rho_2}}$ from the $\rho_2$th column of $|\widehat{\Omega}|$, where $\rho_2 = 1, 2, \ldots, \omega-1$, then obtain

$$\lim_{t\to+\infty} |\widehat{\Omega}| = (-2)^N e^{4(\theta_{1,\mathrm{R}}+\theta_{2,\mathrm{R}}+\cdots+\theta_{\omega-1,R})} |\widehat{\Omega}^{+}|,$$
$$|\widehat{\Omega}^{+}| = \begin{vmatrix} \frac{1}{\lambda_1^*-\lambda_1} & \cdots & \frac{1}{\lambda_1^*-\lambda_{\omega-1}} & \frac{e^{2\theta_\omega}}{\lambda_1^*-\lambda_\omega} & 0 & \cdots & 0 \\ \vdots & \ddots & \vdots & \vdots & \vdots & \ddots & \vdots \\ \frac{1}{\lambda_{\omega-1}^*-\lambda_1} & \cdots & \frac{1}{\lambda_{\omega-1}^*-\lambda_{\omega-1}} & \frac{e^{2\theta_\omega}}{\lambda_{\omega-1}^*-\lambda_\omega} & 0 & \cdots & 0 \\ \frac{e^{2\theta_\omega^*}}{\lambda_\omega^*-\lambda_1} & \cdots & \frac{e^{2\theta_\omega^*}}{\lambda_\omega^*-\lambda_{\omega-1}} & \frac{e^{2(\theta_\omega^*+\theta_\omega)}+1}{\lambda_\omega^*-\lambda_\omega} & \frac{1}{\lambda_\omega^*-\lambda_{\omega+1}} & \cdots & \frac{1}{\lambda_\omega^*-\lambda_N} \\ 0 & \cdots & 0 & \frac{1}{\lambda_{\omega+1}^*-\lambda_\omega} & \frac{1}{\lambda_{\omega+1}^*-\lambda_{\omega+1}} & \cdots & \frac{1}{\lambda_{\omega+1}^*-\lambda_N} \\ \vdots & \ddots & \vdots & \vdots & \vdots & \ddots & \vdots \\ 0 & \cdots & 0 & \frac{1}{\lambda_N^*-\lambda_\omega} & \frac{1}{\lambda_N^*-\lambda_{\omega+1}} & \cdots & \frac{1}{\lambda_N^*-\lambda_N} \end{vmatrix}. \tag{13}$$

We operate the same procedure for $\begin{vmatrix} \widehat{\Omega} & \widehat{X}_3^{\dagger} \\ \widehat{X}_1 & 0 \end{vmatrix}$ as the above $|\widehat{\Omega}|$, and obtain

$$\lim_{t\to+\infty} \begin{vmatrix} \widehat{\Omega} & \widehat{X}_3^{\dagger} \\ \widehat{X}_1 & 0 \end{vmatrix} = (-2)^{N-1} e^{4(\theta_{1,\mathrm{R}}+\theta_{2,\mathrm{R}}+\cdots+\theta_{\omega-1,R})} \cdot \begin{vmatrix} \widehat{\Omega}^{+} & (\widehat{X}_3^{+})^{\dagger} \\ \widehat{X}_1^{+} & 0 \end{vmatrix},$$
$$\widehat{X}_1^{+} = \Big(\underbrace{1, \ldots, 1}_{\omega-1}, e^{2\theta_\omega}, \underbrace{0, \ldots, 0}_{N-\omega}\Big),$$
$$(\widehat{X}_3^{+})^{\dagger} = \Big(\underbrace{0, \ldots, 0}_{\omega-1}, 1, \ldots, 1\Big)^{\mathrm{T}}. \tag{14}$$

Similarly, when $t \to +\infty$, we finally obtain the expression of the $\omega$th asymptotic soliton component as

$$|\phi_1[N]| = |\phi_0[N]| = |\phi_{-1}[N]|$$
$$= |\lambda_{\omega,C}| \operatorname{sech}\Big(2\theta_{\omega,R} - \frac{1}{2}\ln\Upsilon_\omega\Big). \tag{15}$$

Asymptotic solitons (12) and (15) represent the asymptotic expressions for the $\omega$th soliton component as $t \to \pm\infty$. Thus, we have derived the complete asymptotic expressions of the $N$ soliton components in $N$-soliton solutions (5). Based on asymptotic solitons (12) and (15), we summarize the following physical properties of the multiple matter-wave solitons in the spinor BECs:

(I) All the matter-wave soliton components are bright-type, representing the localized regions of the higher density that form in the spinor BECs with the attractive interactions. The amplitude of the $\omega$th matter-wave soliton component is always $\lambda_{\omega,C}$. During the propagation and interactions, each matter-wave soliton component maintains its amplitude. The above analysis indicates that the matter-wave solitons in the spinor BECs possess the property of maintaining their energy content and coherence during the propagation and interactions.

(Ⅱ) During the multiple matter-wave soliton interactions, each matter-wave soliton component interacts with the other $N-1$ matter-wave soliton components, i.e., each matter-wave soliton component undergoes $N-1$ interactions. Before and after the $N-1$ matter-wave soliton interactions, the $\omega$th matter-wave soliton component only encounters a phase shift of $|\ln\Upsilon_\omega|$. It is important to note that the phase shift is relevant with the other $N-1$ spectral parameters, but is independent of the space and time variables $x$ and $t$. Therefore, we can infer that every matter-wave soliton component contributes to the phase shifts of the other matter-wave soliton components.

(Ⅲ) Characteristic line of the $\omega$th matter-wave soliton

component before the $N-1$ interactions: $2\theta_{\omega,R}+\frac{1}{2}\ln\Upsilon_\omega = 0$. Characteristic line of the $\omega$th matter-wave soliton component after the $N-1$ interactions: $2\theta_{\omega,R}-\frac{1}{2}\ln\Upsilon_\omega = 0$. Width of the $\omega$-th matter-wave soliton is $1/(1+16\lambda^2_{\omega,R})$.

(Ⅳ) Since before and after the interactions, those $N$ matter-wave soliton components pass through each other without any change in shape, width, amplitude or velocity, and hence there is no energy transfer between those matter-wave solitons, we infer that those matter-wave soliton interactions are elastic. In other words, the matter-wave solitons in the spinor BECs admit elastic interactions.

To verify the correctness of the above asymptotic results, we take $N=3$ in $N$-soliton solutions (5) as an example. When $N=3$, we provide the three spectral parameters as $\lambda_1=\frac{1}{2}+\frac{1}{2}i$, $\lambda_2=i$, $\lambda_3=-\frac{1}{4}+\frac{1}{2}i$. Since $\lambda_{1,\mathrm{C}}>0$, $\lambda_{2,\mathrm{C}}>0$, $\lambda_{3,\mathrm{C}}>0$ and $\lambda_{1,\mathrm{R}}>\lambda_{2,\mathrm{R}}>\lambda_{3,\mathrm{R}}$, substituting the three spectral parameters into asymptotic solitons (12) and (15), we calculate the following expressions of the three asymptotic matter-wave solitons as

$$\begin{aligned}
S_1^{\pm}:\ &|\phi_1[3]| = |\phi_0[3]| \\
&= |\phi_{-1}[3]| \to \frac{1}{2}\mathrm{sech}\Big[\frac{1}{2}(x+2t)\pm\frac{1}{2}\ln\frac{125}{9}\Big], \\
S_2^{\pm}:\ &|\phi_1[3]| = |\phi_0[3]| \\
&= |\phi_{-1}[3]| \to 1\mathrm{sech}\Big[x\pm\frac{1}{2}\ln\frac{37}{25}\Big], \\
S_3^{\pm}:\ &|\phi_1[3]| = |\phi_0[3]| \\
&= |\phi_{-1}[3]| \to \frac{1}{2}\mathrm{sech}\Big[\frac{1}{2}(x-t)\pm\frac{1}{2}\ln\frac{9}{185}\Big].
\end{aligned} \tag{16}$$

Asymptotic expressions (16) indicate that: Amplitudes of $S_1^{\pm}$ and $S_3^{\pm}$ are $\frac{1}{2}$, while amplitudes of $S_2^{\pm}$ are 1. At any time, phase shifts between $S_1^+$ and $S_1^-$, $S_2^+$ and $S_2^-$, $S_3^+$ and $S_3^-$ are $\ln\frac{125}{9}$, $\ln\frac{37}{25}$, $\ln\frac{9}{185}$, respectively. The three soliton interactions are elastic.

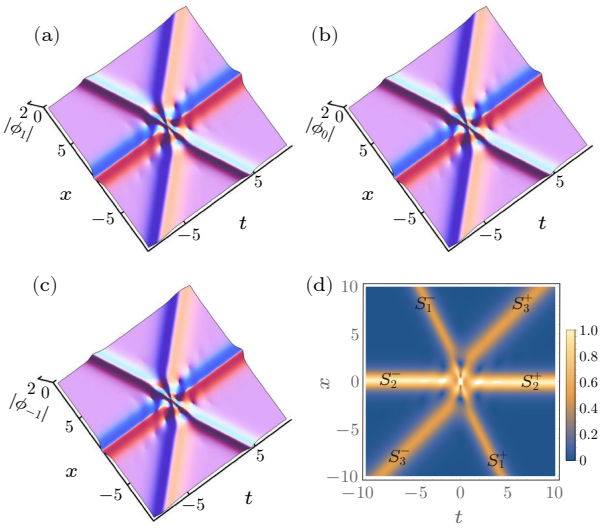


**Fig. 1.** For the three interacting matter-wave solitons via $N$-soliton solutions (5) with $N=3$, $\lambda_1=\frac{1}{2}+\frac{1}{2}i$, $\lambda_2=i$, $\lambda_3=-\frac{1}{4}+\frac{1}{2}i$: [(a), (b), (c)] 3D plots. (d) The corresponding density plot.

We depict the three-dimensional (3D) plots of the three interacting matter-wave solitons in Figs. 1(a), 1(b), and 1(c), and illustrate the density plot of the three interacting matter-wave solitons in Fig. 1(d). Those figures are consistent with the properties of the interacting matter-wave solitons obtained above.

*Triple-Pole Soliton Asymptotics and Corresponding Example Verification.* Multi-pole solitons, typically derived using the generalized DT method, exhibit distinct properties compared to the normal solitons, including curved characteristic lines and stable attractive forces between different soliton components. External trapping potentials, such as magnetic or optical traps, play a crucial role in shaping multi-pole matter-wave solitons in BECs. Those potentials provide the necessary confinement for solitons to maintain their shape and coherence over extended distances.

To obtain the multi-pole solitons for system (2), we introduce the following Taylor expansion method based on the binary DT method. Firstly, we add a small parameter $\epsilon$ to a spectral parameter $\lambda_1$. On the zero background $\phi_{-1}=\phi_0=\phi_1=0$, eigenfunction of Lax Pair (3) at the complex spectral parameter $\lambda=\lambda_1(1+\epsilon)$ can be expressed as

$$\begin{aligned}
\Gamma_1 &= \begin{pmatrix}\gamma_{1,1}\\ \gamma_{2,1}\\ \gamma_{3,1}\\ \gamma_{4,1}\end{pmatrix} = \begin{pmatrix} e^{-i\lambda_1(1+\epsilon)x-2i\lambda_1^2(1+\epsilon)^2t}\\ e^{-i\lambda_1(1+\epsilon)x-2i\lambda_1^2(1+\epsilon)^2t}\\ e^{i\lambda_1(1+\epsilon)x+2i\lambda_1^2(1+\epsilon)^2t}\\ e^{i\lambda_1(1+\epsilon)x+2i\lambda_1^2(1+\epsilon)^2t}\end{pmatrix} \\
&= \Lambda_0+\Lambda_1\epsilon+\Lambda_2\epsilon^2+\cdots, \\
\Lambda_0 &= \begin{pmatrix} e^{\theta_1}\\ e^{\theta_1}\\ e^{-\theta_1}\\ e^{-\theta_1}\end{pmatrix}, \quad \Lambda_1 = \begin{pmatrix} -i\lambda_1(x+4\lambda_1 t)e^{\theta_1}\\ -i\lambda_1(x+4\lambda_1 t)e^{\theta_1}\\ i\lambda_1(x+4\lambda_1 t)e^{-\theta_1}\\ i\lambda_1(x+4\lambda_1 t)e^{-\theta_1}\end{pmatrix}, \\
\Lambda_2 &= \begin{pmatrix} -\frac{1}{2}\lambda_1^2[4it+(x+4\lambda_1 t)^2]e^{\theta_1}\\ -\frac{1}{2}\lambda_1^2[4it+(x+4\lambda_1 t)^2]e^{\theta_1}\\ \frac{1}{2}\lambda_1^2[4it-(x+4\lambda_1 t)^2]e^{-\theta_1}\\ \frac{1}{2}\lambda_1^2[4it-(x+4\lambda_1 t)^2]e^{-\theta_1}\end{pmatrix},
\end{aligned} \tag{17}$$

where $\theta_1=-i\lambda_1 x-i\lambda_1^2 t$, and $\epsilon$ is a complex small parameter, i.e., $\lambda^*=\lambda_1^*(1+\epsilon^*)$.

Then, we present the tripe-pole soliton solutions as

$$\begin{aligned}
\phi_1[3] &= 2i\frac{\begin{vmatrix}\Omega & G_3^\dagger\\ G_1 & 0\end{vmatrix}}{|\Omega|}, \quad \phi_0[3] = 2i\frac{\begin{vmatrix}\Omega & G_4^\dagger\\ G_1 & 0\end{vmatrix}}{|\Omega|}, \\
\phi_{-1}[3] &= 2i\frac{\begin{vmatrix}\Omega & G_4^\dagger\\ G_2 & 0\end{vmatrix}}{|\Omega|},
\end{aligned} \tag{18}$$

where $G=(\Lambda_0,\Lambda_1,\Lambda_2)$; $G_1$, $G_2$, $G_3$, $G_4$ are the 1st, 2nd, 3rd, 4th rows of $G$, respectively, and $\Omega=(\Omega_{j,k})_{3\times3}$ with

$$\frac{\Gamma_1^\dagger\Gamma_1}{\lambda_1-\lambda_1^*} = \sum_{j=1,k=1}^{+\infty,+\infty}\Omega_{j,k}(\epsilon^*)^{j-1}\epsilon^{k-1}. \tag{19}$$

Actually, we can obtain the detailed expressions of $\Omega_{j,k}$ as

follows:

$$\Omega_{j,k} = \sum_{m=0}^{j+k-2} \sum_{l=\max(0,\,m-j+1)}^{\min(k-1,\,m)} \Big(\frac{1}{\lambda_1-\lambda_1^*}\Big)^{m+1} \cdot C_m^l \lambda_1^{*m-l}(-\lambda_1)^l \Lambda_{j-1-m+l}^{\dagger} \Lambda_{k-1-l}. \tag{20}$$

It should be noted that the above results have been significantly simplified. Hence, we simplify solutions (18) to the following triple-pole soliton solutions:

$$\begin{aligned}
\phi_1[3] &= \phi_0[3] = \phi_{-1}[3] \\
&= -2\lambda_{1,\mathrm{C}} e^{2i\theta_{1,\mathrm{C}}} \\
&\quad \cdot \frac{\Delta_1 e^{4\theta_{1,\mathrm{R}}} + \Delta_2 e^{-4\theta_{1,\mathrm{R}}} + \Delta_3}{e^{6\theta_{1,\mathrm{R}}} + e^{-6\theta_{1,\mathrm{R}}} + \Delta_4 e^{2\theta_{1,\mathrm{R}}} + \Delta_5 e^{-2\theta_{1,\mathrm{R}}}}, \\
\Delta_1 &= 128\lambda_{1,\mathrm{C}}^4 t^2 - 8\theta_{1,\mathrm{R}}^2 + (64i\lambda_{1,\mathrm{C}}^2 t + 12)\theta_{1,\mathrm{R}} \\
&\quad - 64i\lambda_{1,\mathrm{C}}^2 t - 3, \\
\Delta_2 &= 128\lambda_{1,\mathrm{C}}^4 t^2 - 8\theta_{1,\mathrm{R}}^2 - (64i\lambda_{1,\mathrm{C}}^2 t + 12)\theta_{1,\mathrm{R}} \\
&\quad - 64i\lambda_{1,\mathrm{C}}^2 t - 3, \\
\Delta_3 &= 8192\lambda_{1,\mathrm{C}}^8 t^4 + 32\theta_{1,\mathrm{R}}^4 + (16 + 1024\lambda_{1,\mathrm{C}}^4 t^2 \\
&\quad - 256i\lambda_{1,\mathrm{C}}^2 t)\theta_{1,\mathrm{R}}^2 + 128\lambda_{1,\mathrm{C}}^4 t^2 - 64i\lambda_{1,\mathrm{C}}^2 t - 3, \\
\Delta_4 &= 16384\lambda_{1,\mathrm{C}}^8 t^4 + 64\theta_{1,\mathrm{R}}^4 - 64\theta_{1,\mathrm{R}}^3 \\
&\quad + (48 + 2048\lambda_{1,\mathrm{C}}^4 t^2)\theta_{1,\mathrm{R}}^2 - 3072\lambda_{1,\mathrm{C}}^4 t^2 \theta_{1,\mathrm{R}} \\
&\quad + 1536\lambda_{1,\mathrm{C}}^4 t^2 + 3, \\
\Delta_5 &= 16384\lambda_{1,\mathrm{C}}^8 t^4 + 64\theta_{1,\mathrm{R}}^4 + 64\theta_{1,\mathrm{R}}^3 \\
&\quad + (48 + 2048\lambda_{1,\mathrm{C}}^4 t^2)\theta_{1,\mathrm{R}}^2 + 3072\lambda_{1,\mathrm{C}}^4 t^2 \theta_{1,\mathrm{R}} \\
&\quad + 1536\lambda_{1,\mathrm{C}}^4 t^2 + 3, \\
\theta_{1,\mathrm{R}} &= \lambda_{1,\mathrm{C}}(x + 4\lambda_{1,\mathrm{R}} t), \\
\theta_{1,\mathrm{C}} &= -\lambda_{1,\mathrm{R}} x + 2(\lambda_{1,\mathrm{C}}^2 - \lambda_{1,\mathrm{R}}^2)t.
\end{aligned} \tag{21}$$

For triple-pole solitons (21), we aim to deduce the expressions of the three asymptotic soliton components $S_1$, $S_2$, and $S_3$. Triple-pole solutions (21) consist of a line-type soliton component and two curve-type soliton components.

Along the characteristic line $\theta_{1,\mathrm{R}} = \text{const}$ to $t \to \pm\infty$, we neglect the infinitesimal quantities and only retain the $t^4$ terms in the numerators and denominators of $\phi_1[3]$, $\phi_0[3]$, $\phi_{-1}[3]$, finally work out the asymptotic expressions of the single line-type soliton component $S_2$,

$$\begin{aligned}
&|\phi_1[3]| = |\phi_0[3]| = |\phi_{-1}[3]| = |\lambda_{1,\mathrm{C}}|\ \mathrm{sech}(2\theta_{1,\mathrm{R}}), \\
&\theta_{1,\mathrm{R}} = \text{const},\ t \to \pm\infty.
\end{aligned} \tag{22}$$

As to the two curve-type soliton components, we consider the balances between $e^{\theta_{1,\mathrm{R}}}$ and $t$ as $t \propto e^{\theta_{1,\mathrm{R}}}$ or $t \propto e^{-\theta_{1,\mathrm{R}}}$ and obtain:

When $t \propto e^{\theta_{1,\mathrm{R}}}$, $\theta_{1,\mathrm{R}} \to +\infty$, $t \to \pm\infty$,

$$\begin{aligned}
&|\phi_1[3]| = |\phi_0[3]| = |\phi_{-1}[3]| \to S_1^+, \\
&S_3^- = |\lambda_{1,\mathrm{C}}| e^{i\Lambda} \mathrm{sech}(2\theta_{1,\mathrm{R}} - \ln 128\lambda_{1,\mathrm{C}}^4 t^2);
\end{aligned} \tag{23}$$

When $t \propto e^{-\theta_{1,\mathrm{R}}}$, $\theta_{1,\mathrm{R}} \to -\infty$, $t \to \pm\infty$.

$$\begin{aligned}
&|\phi_1[3]| = |\phi_0[3]| = |\phi_{-1}[3]| \to S_3^+, \\
&S_1^- = |\lambda_{1,\mathrm{C}}| e^{i\Lambda} \mathrm{sech}(2\theta_{1,\mathrm{R}} + \ln 128\lambda_{1,\mathrm{C}}^4 t^2).
\end{aligned} \tag{24}$$

According to asymptotic solitons (22), (23), and (24), we get the asymptotic trajectories of the three bright-type asymptotic soliton components as

$$\begin{aligned}
&S_1^+,\ S_3^-:\ 128\lambda_{1,\mathrm{C}}^4 t^2 - e^{2\theta_{1,\mathrm{R}}} = 0, \\
&S_2^{\pm}:\ \theta_{1,\mathrm{R}} = 0, \\
&S_3^+,\ S_1^-:\ 128\lambda_{1,\mathrm{C}}^4 t^2 - e^{-2\theta_{1,\mathrm{R}}} = 0,
\end{aligned} \tag{25}$$

along which $S_1$, $S_2$, and $S_3$ reach their respective maxima. The corresponding slopes of $S_1$, $S_2$, and $S_3$ in the $x$–$t$ plane can be obtained as follows:

$$\begin{aligned}
&S_1^+:\ -4\lambda_{1,\mathrm{R}} + \frac{1}{\lambda_{1,\mathrm{C}} t} \quad (t > 0), \\
&S_1^-:\ -4\lambda_{1,\mathrm{R}} - \frac{1}{\lambda_{1,\mathrm{C}} t} \quad (t < 0), \\
&S_2:\ -4\lambda_{1,\mathrm{R}}, \\
&S_3^+:\ -4\lambda_{1,\mathrm{R}} - \frac{1}{\lambda_{1,\mathrm{C}} t} \quad (t > 0), \\
&S_3^-:\ -4\lambda_{1,\mathrm{R}} + \frac{1}{\lambda_{1,\mathrm{C}} t} \quad (t < 0).
\end{aligned} \tag{26}$$

Since the slopes of $S_1^{\pm}$ and $S_3^{\pm}$ all approach to $-4\lambda_{1,\mathrm{R}}$ asymptotically when $t \to \pm\infty$, we infer that the center trajectories of $S_1^{\pm}$ and $S_3^{\pm}$ are approximately parallel to $l_1$ as $t \to \pm\infty$. At $x = t = 0$, $|\phi_1[3]|$, $|\phi_0[3]|$, and $|\phi_{-1}[3]|$ reach their global maxima $3|\lambda_{1,\mathrm{C}}|$, which is three times the amplitude of the single asymptotic soliton components.

For the properties of the matter-wave soliton interactions, we can conclude the following two aspects:

(i) Phase shift between $S_1^-$ and $S_1^+$ is $P_1 = -4\ln 8\sqrt{2}\lambda_{1,\mathrm{C}}^2 |t|$, phase shift between $S_3^-$ and $S_3^+$ is $P_3 = 4\ln 8\sqrt{2}\lambda_{1,\mathrm{C}}^2 |t|$, while there is no phase shift between $S_2^-$ and $S_2^+$. In view of $P_1$ and $P_3$ being opposite under the same $|t|$, and the slope of $S_1^+$ (or $S_3^+$) at $t$ is equal to that of $S_1^-$ (or $S_3^-$) at $-t$, we judge that triple-pole solitons (21) describe the elastic interactions between the two curve-type matter-wave soliton components while the line-type matter-wave soliton component remains unchanged.

(ii) For the relative distance between the adjacent matter-wave soliton components, we have $D_{12} = D_{23} = \frac{\ln 8\sqrt{2}\lambda_{1,\mathrm{C}}^2 |t|}{|\lambda_{1,\mathrm{C}}|}$, which grows logarithmically with $|t|$. Moreover, we calculate the second derivative of $D_{12}$ with respect to time $|t|$ as $A_{12} = -128\lambda_{1,\mathrm{C}}^3 e^{-2\lambda_{1,\mathrm{C}} D_{12}}$, which indicates that the separation acceleration between the adjacent matter-wave solitons decreases exponentially with the relative distance and finally approaches 0. This point indicates the stable attractive forces between the different matter-wave soliton components.

Triple-pole matter-wave solitons can be regarded as a combination of the double-pole matter-wave solitons and a single matter-wave soliton. Indeed, another type of third-order matter-wave solitons, consisting of double-pole matter-wave solitons and a single matter-wave soliton, can also be derived, involving two spectral parameters. However, it is essential to clarify that the central matter-wave soliton component in the triple-pole matter-wave solitons does not undergo a phase shift, whereas the single matter-wave soliton component in other types of third-order matter-wave solitons does undergo a phase shift.

Additionally, the balance condition for triple-pole matter-wave solitons differs from that for double-pole matter-wave solitons.

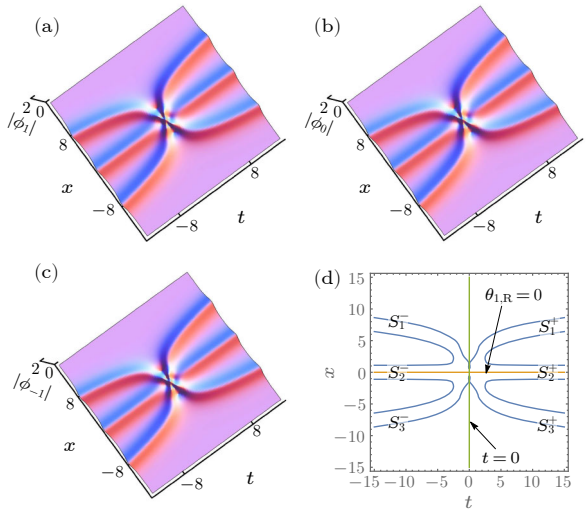


**Fig. 2.** For the triple-pole matter-wave solitons via triple-pole solitons (21) with $\lambda_1 = \frac{1}{2}i$: [(a), (b), (c)] 3D plots. (d) The corresponding contour plot.

In Fig. 2, we illustrate the triple-pole matter-wave solitons and mark the asymptotic solitons in the contour figure. It can be seen that Fig. 2 is consistent with the above asymptotic-soliton properties.

*Dynamical Stability Analysis for the Multiple Solitons.* Numerous nonlinear processes exhibit an instability in the modulation of the steady state due to the interaction of nonlinear and dispersive effects. Next, we analyze the modulation instability of system (2) using linear stability techniques.

Since the multiple solitons discussed in this study appear on a zero background, we assume the perturbed nonlinear background as

$$\begin{aligned}
\phi_{-1} &= 0 + \epsilon[P_{-1}e^{i\eta x+\kappa t} + iQ_{-1}e^{i\eta x+\kappa t}],\\
\phi_0 &= 0 + \epsilon[P_0 e^{i\eta x+\kappa t} + iQ_0 e^{i\eta x+\kappa t}],\\
\phi_1 &= 0 + \epsilon[P_1 e^{i\eta x+\kappa t} + iQ_1 e^{i\eta x+\kappa t}],
\end{aligned} \tag{27}$$

where $\epsilon$ is a small parameter, $\eta$ is an arbitrary real wave number of the small perturbation, $\kappa$ is the modulation instability gain (generally speaking, this eigenvalue may be complex), $P_{-1}$, $Q_{-1}$, $P_0$, $Q_0$, $P_1$, and $Q_1$ are the real constant amplitudes of the perturbation eigenmode. By substituting expressions (27) into system (2), neglecting $o(\epsilon)$, and separating the real part from the imaginary part, we obtain a linear homogeneous system of $P_{-1}$, $Q_{-1}$, $P_0$, $Q_0$, $P_1$, and $Q_1$ as

$$\begin{aligned}
&\eta^2 P_{-1} + \kappa Q_{-1} = 0, \quad -\kappa P_{-1} + \eta^2 Q_{-1} = 0,\\
&\eta^2 P_0 + \kappa Q_0 = 0, \quad -\kappa P_0 + \eta^2 Q_0 = 0,\\
&\eta^2 P_1 + \kappa Q_1 = 0, \quad -\kappa P_1 + \eta^2 Q_1 = 0.
\end{aligned} \tag{28}$$

Since $P_{-1}$, $Q_{-1}$, $P_0$, $Q_0$, $P_1$, and $Q_1$ are not all zero, we find the following condition:

$$\begin{vmatrix} \eta^2 & \kappa \\ -\kappa & \eta^2 \end{vmatrix} = 0, \tag{29}$$

which generates the relation $\kappa^2 = -\eta^4$. This relation $\kappa^2 = -\eta^4$ governs the connection between time oscillations $e^{\kappa t}$ and spatial oscillations $e^{i\eta x}$ with a wave number $\eta$. As $\kappa^2$ is consistently non-positive, modulation instability is absent, indicating that the soliton solutions for system (2) exhibit dynamic stability against minor perturbations.

In conclusions, a (1+1)-dimensional three-couple GP system, i.e., system (2), which depicts the macroscopic spinor BEC waves within the mean-field approximation, has been investigated. With respect to the distribution of atoms corresponding to the three vertical spin projections $m_{\rm F} = 1, 0, -1$, we have firstly derived $N$-soliton solutions (5) in the determinant form and then performed the asymptotic analysis on $N$-soliton solutions (5) to obtain the entire asymptotic expressions of the $N$ matter-wave soliton components as asymptotic solitons (12) and (15). Moreover, triple-pole solitons (21) have also been obtained and analyzed, which lead to asymptotic expressions asymptotic solitons (22)–(24). Those asymptotic results have indicated that: The matter-wave solitons in the spinor BECs exhibit the property of maintaining their energy content and coherence during the propagation and interactions. In the $N$ matter-wave solitons, each matter-wave soliton component contributes to the phase shifts of the other soliton components. In the triple-pole matter-wave solitons, stable attractive forces exist between the different matter-wave soliton components. Via the 3D plots, density plot and contour plot, we have verified the asymptotic-analysis results of the $N$ solitons and triple-pole solitons, as shown in Figs. 1 and 2, respectively.

We believe that our analysis results may not only offer the explanations for the complex natural mechanisms of the matter waves in the spinor BECs, but also have the potential applications in designs of atom lasers, atom interferometry and coherent atom transport.

*Acknowledgements.* This work was supported by the National Natural Science Foundation of China (Grant No. 12161061), the Fundamental Research Funds for the Inner Mongolia University of Finance and Economics (Grant No. NCYWT23036), the Young innovative and Entrepreneurial Talents of the Inner Mongolia Grassland Talents Project in 2022, Autonomous Region "Five Major Tasks" Research Special Project for the Inner Mongolia University of Finance and Economics in 2024 (Grant No. NCXWD2422), High Quality Research Achievement Cultivation Fund for the Inner Mongolia University of Finance and Economics in 2024 (Grant No. GZCG2426), and the Talent Development Fund of Inner Mongolia.

# References

[1] Wang B 2023 *Highlights Sci. Eng. Technol.* **38** 19
[2] Zhou Q 2022 *Chin. Phys. Lett.* **39** 010501
[3] Liu C, Chen S C, Yao X K, and Akhmediev N 2022 *Chin. Phys. Lett.* **39** 094201
[4] Bagnato V S, Frantzeskakis D J, Kevrekidis P G, Malomed B A, and Mihalache D 2015 *Rom. Rep. Phys.* **67** 5
[5] Mihalache D 2024 *Rom. Rep. Phys.* **76** 402

[6] Kevrekidis P G, Frantzeskakis D J, and Carretero-González R 2008 *Emergent Nonlinear Phenomena in Bose–Einstein Condensates: Theory And Experiment* (Berlin: Springer-Verlag)
[7] Yan L J, Liu Y J, and Hu X B 2024 *Chin. Phys. Lett.* **41** 040201
[8] Kawaguchi Y, and Ueda M 2012 *Phys. Rep.* **520** 253
[9] Wazwaz A M 2023 *Chin. Phys. Lett.* **40** 120501
[10] Liu X M, Zhang Z Y, and Liu W J 2023 *Chin. Phys. Lett.* **40** 070501
[11] Ma W X 2022 *Chin. Phys. Lett.* **39** 100201
[12] Lou S Y, Jia M, and Hao X Z 2023 *Chin. Phys. Lett.* **40** 020201
[13] Kengne E, Liu W M, and Malomed B A 2021 *Phys. Rep.* **899** 1
[14] Musolino S, Kurkjian H, Van Regemortel M, Wouters M, Kokkelmans S J J M F, and Colussi V E 2022 *Phys. Rev. Lett.* **128** 020401
[15] Henderson G W, Robb G R M, Oppo G L, and Yao A M 2022 *Phys. Rev. Lett.* **129** 073902
[16] Krzyzanowska K A, Ferreras J, Ryu C, Samson E C, and Boshier M G 2023 *Phys. Rev. A* **108** 043305
[17] Xu S, Schmiedmayer J, and Sanders B C 2022 *Phys. Rev. Res.* **4** 023071
[18] Dąbrowska-Wüster B J, Ostrovskaya E A, Alexander T J, and Kivshar Y S 2007 *Phys. Rev. A* **75** 023617
[19] Wang Y H, Meng L Z, and Zhao L C 2024 *Commun. Theor. Phys.* **76** 065006
[20] Stamper-Kurn D M, Andrews M R, Chikkatur A P, Inouye S, Miesner H J, Stenger J, and Ketterle W 1998 *Phys. Rev. Lett.* **80** 2027
[21] Borgh M O, Lovegrove J, and Ruostekoski J 2017 *Phys. Rev. A* **95** 053601
[22] Kivioja M, Zamora-Zamora R, Blinova A, Mönkölä S, Rossi T, and Möttönen M 2023 *Phys. Rev. Res.* **5** 023104
[23] Ollikainen T, Masuda S, Möttönen M, and Nakahara M 2017 *Phys. Rev. A* **95** 013615
[24] Ding C C, Zhou Q, Xu S L, Sun Y Z, Liu W J, Mihalache D, and Malomed B A 2023 *Chaos Solitons Fract.* **169** 113247
[25] Ding C C, Zhou Q, Xu S L, Triki H, Mirzazadeh M, and Liu W J 2023 *Chin. Phys. Lett.* **40** 040501
[26] Li S, Prinari B, and Biondini G 2018 *Phys. Rev. E* **97** 022221
[27] Li L, Li Z, Malomed B A, Mihalache D, and Liu W M 2005 *Phys. Rev. A* **72** 033611
[28] Qin Z Y and Mu G 2012 *Phys. Rev. E* **86** 036601
[29] Ieda J, Miyakawa T, and Wadati M 2004 *Phys. Rev. Lett.* **93** 194102
[30] Ieda J, Miyakawa T, and Wadati M 2004 *J. Phys. Soc. Jpn.* **73** 2996
[31] He J T, Fang P P, and Lin J 2022 *Chin. Phys. Lett.* **39** 020301
[32] Zhang C R, Tian B, Qu Q X, Yuan Y Q, and Wei C C 2022 *Commun. Nonlinear Sci. Numer. Simulat.* **109** 105988
[33] Luo X 2020 *Chaos Solitons Fract.* **131** 109479
[34] Wen X Y, Lin Z, and Wang D S 2024 *Phys. Rev. E* **109** 044215
[35] Sun W R, and Wang L 2018 *Porc. R. Soc. A* **474** 20170276
[36] Prinari B, Demontis F, Li S, and Horikis T P 2018 *Physica D* **368** 22
[37] Loomba S 2015 *Int. J. Mod. Phys. B* **29** 1550125
[38] Geng X, Wang K, and Chen M 2021 *Commun. Math. Phys.* **382** 585
[39] Sanz J, Frölian A, Chisholm C S, Cabrera C R, and Tarruell L 2022 *Phys. Rev. Lett.* **128** 013201
[40] Fang P, and Lin J 2024 *Phys. Rev. E* **109** 064219
[41] Wang W, Zhao L C, Charalampidis E G, and Kevrekidis P G 2021 *J. Phys. B* **54** 055301
[42] Romero-Ros A, Katsimiga G C, Kevrekidis P G, Prinari B, Biondini G, and Schmelcher P 2021 *Phys. Rev. A* **103** 023329
[43] Yang J, and Zhang Y 2023 *Phys. Rev. A* **107** 023316
[44] Sekh G A, Pepe F V, Facchi P, Pascazio S, and Salerno M 2015 *Phys. Rev. A* **92** 013639
[45] Chai X, Lao D, Fujimoto K, Hamazaki R, Ueda M, and Raman C 2020 *Phys. Rev. Lett.* **125** 030402
[46] Chen Y, Wu Z, Xiao P, Xiao W, and Liu W 2024 *Opt. Lett.* **49** 2437
[47] Xing X, Liu Y, Han J, Liu W, and Wei Z 2023 *ACS Photon.* **10** 2264
[48] Liu W, Xiong X, Liu M, Xing X, Chen H, Ye H, Han J, and Wei Z 2022 *Appl. Phys. Lett.* **120** 053108
[49] Liu M L, Wu H B, Liu X M, Wang Y R, Lei M, Liu W J, Guo W, and Wei Z Y 2021 *Opto-Electron. Adv.* **4** 200029
[50] Zhao X H 2024 *Appl. Math. Lett.* **149** 108895
[51] Zhong Y, Triki H, and Zhou Q 2024 *Chin. Phys. Lett.* **41** 070501